Toroidal nature of the low-energy $E1$ mode

A. Repko,[1] P.-G. Reinhard,[2] V. O. Nesterenko,[3,*] and J. Kvasil[1]
[1]*Institute of Particle and Nuclear Physics, Charles University, CZ-18000, Praha 8, Czech Republic*
[2]*Institut für Theoretische Physik II, Universität Erlangen, D-91058 Erlangen, Germany*
[3]*Laboratory of Theoretical Physics, Joint Institute for Nuclear Research, Dubna, Moscow region 141980, Russia*
(Received 10 December 2012; published 6 February 2013)

The nature of $E1$ low-energy strength (LES), often denoted as a "pygmy dipole resonance", is analyzed within the random-phase approximation (RPA) in ^{208}Pb using Skyrme forces in a fully self-consistent manner. A first overview is given by the strength functions for the dipole, compressional, and toroidal operators. More detailed insight is gained by averaged transition densities and currents where the latter provide a very illustrative flow pattern. The analysis reveals clear isoscalar toroidal flow in the low-energy bin 6.0–8.8 MeV of the LES and a mixed isoscalar/isovector toroidal/compression flow in the higher bin 8.8–10.5 MeV. Thus the modes covered by LES embrace both vortical and irrotational motion. The simple collective picture of the LES as a "pygmy" mode (oscillations of the neutron excess against the nuclear core) is not confirmed.

DOI: 10.1103/PhysRevC.87.024305 PACS number(s): 24.30.Cz, 21.60.Jz, 27.80.+w

I. INTRODUCTION

During the last decade we observe an increasing interest in low-energy $E1$ strength (LES), for a recent review see [1]. This interest is caused by a possible relation of LES to the neutron skin in nuclei and density dependence of the nuclear symmetry energy. This in turn may be important for building the isospin-dependent part of the nuclear equation of state and various astrophysical applications [2]. Several different views of the LES origin come together. Most often the LES is interpreted as a "pygmy dipole resonance" (PDR) modeled as the oscillation of the neutron excess against the nuclear core [1,3–5]. There are, however, serious objections against such a simplistic collective picture [6,7]. In fact, the landscape of LES may be much richer. It can embrace also the toroidal resonance (TR) [8,9] and anisotropic compression resonance (CR) [10,11] both of which are of actual interest [1]. After exclusion of nuclear center-of-mass (c.m.) motion, the TR and CR dominate in the isoscalar ($T = 0$) channel and constitute the low- and high-energy branches of the isoscalar giant dipole resonance (ISGDR). Following recent microscopic studies [12,13], TR dominates in the LES region and CR, being strongly coupled to TR, also significantly contributes there.

The basic flow patterns of these three modes are shown schematically in Fig. 1. The panels illustrate the PDR oscillations of the neutron skin against the core (a), the typical vortices of TR (b), and the dipole-compressional pattern of CR (c). The latter can be viewed as oscillation of surface against core and thus shares some similarity with the PDR picture of panel (a). Unlike the irrotational PDR and CR, the TR is purely vortical in the hydrodynamical (HD) sense [12,13]. Thus we see that the LES can involve quite different flows, vortical and irrotational.

Despite a great number of publications on PDR, TR, and CR [1], their possible interplay in LES was only occasionally discussed. In particular, the PDR and TR were considered side by side within the quasiparticle-phonon model [14]. It was shown that the vortical strength [15] is peaked in the LES region and the isovector LES velocity field is mainly toroidal. Nevertheless, because of the dominant contribution of the neutron skin to the surface transition density and thus to $B(E1, T = 1)$, the familiar PDR picture of LES was maintained [14]. Similar arguments in favor of the PDR treatment were presented earlier in relativistic [4] and Skyrme [5] mean-field calculations, and taken up in most subsequent publications. Recent explorations questioned the simple PDR-type collectivity of LES [6,7,13], though without analysis of LES velocity fields.

It is the aim of this paper to give a more thorough exploration of the interplay and structure of low-lying dipole modes. The survey is performed using the random-phase approximation (RPA) built on the Skyrme-Hartree-Fock ground state where both, ground state configuration and RPA equations, are derived consistently from the same Skyrme energy functional. To our knowledge, this is the first fully self-consistent study of the PDR/TR interplay. Not only strength functions and transition densities but also the modes' flow patterns will be considered. As we will see, the actual LES flow is predominantly

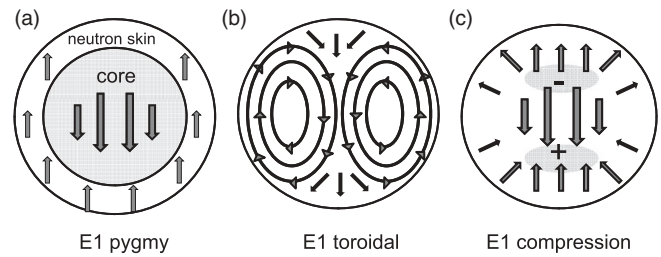

FIG. 1. Schematic velocity fields for the $E1$ pygmy (a), toroidal (b), and high-energy compressional (c) flows. The driving field is directed along the z axis. The arrows indicate only directions of the flows but not their strength. In (c), the compression (+) and decompression (−) regions, characterized by increased and decreased density, are marked.

*nester@theor.jinr.ru

of mixed TR/CR character. This conclusion may have far-reaching consequences for the information content of LES. If vorticity dominates, then only a minor irrotational fraction of LES is relevant for the nuclear symmetry energy and related problems (as was also worked out in the recent correlation analysis [7]).

Note that the previous exploration [14] of the problem was performed within the quasiparticle-phonon model which goes beyond RPA in coupling to complex configurations (CCC). This approach is based on phenomenologically tuned mean-field potential (Woods-Saxon) and residual interaction. Our present study stays at the level of RPA but realizes this in a fully self-consistent manner using a standard Skyrme energy functional. The RPA picture misses the line broadening and structure details of LES [29,30], which are in the scope of CCC. However, we deal with gross features of LES, use the folded RPA spectra, and exploit the average characteristics (transition densities, velocity fields) involving contributions of many RPA states. So the CCC should not considerably affect our results. The more precise CCC treatment would require a thorough revision of the energy functionals [16], which is beyond the scope of the present study.

II. MODEL

Our study is performed for ^{208}Pb using the Skyrme RPA approach with the techniques from Ref. [17]. The method is fully self-consistent as both the mean field and residual interaction are derived from the Skyrme functional [18–20]. The RPA residual interaction takes into account all the terms of the Skyrme functional including the Coulomb (direct and exchange) energy. The center-of-mass correction (c.m.c.) is implemented for the ground state and $T = 0$ dipole excitations. The parametrization SLy6 [21] is used which provides a satisfactory description of $E1(T = 1)$ strength in heavy nuclei [22]. The calculations are done in a one-dimensional (1D) spherical coordinate-space grid with mesh size 0.3 fm and a calculation box of 21 fm.

A large configuration space including $1ph$ states up to $\sim$35 MeV and additional fluid-dynamical basis modes is used. Actually, we employ modes generated by local operators rY_{10}, r^3Y_{10}, and $j_1(qr)Y_{10}$ for a couple of appropriately chosen q where j_1 is the spherical Bessel function of first order. The r^nY_{10} take into account collective surface flow and the $j_1(qr)Y_{10}$ explore volume properties. The chosen set of explicit $1ph$ states together with the fluid-dynamical modes form a nonorthogonal basis. This basis is orthonormalized first and then used in standard manner in the RPA scheme [17]. The admixture of fluid-dynamical modes allows to account for the global polarization effects of higher lying modes up to $\sim$200 MeV [17], correctly single out the c.m. mode (i.e., place it safely below 1 MeV), and fully exhaust the Thomas-Reiche-Kuhn (TRK) sum rule.

The excitation modes are first characterized by their strength function

$$S_\alpha(E1;\omega) = 3\sum_\nu \omega_\nu^l |\langle\Psi_\nu|\hat{M}_\alpha(E10)|\Psi_0\rangle|^2 \zeta(\omega,\omega_\nu), \quad (1)$$

where $\zeta(\omega,\omega_\nu) = \Delta(\omega_\nu)/[2\pi[(\omega-\omega_\nu)^2 + \Delta(\omega_\nu)^2/4]]$ is a Lorentzian weight with energy-dependent smoothing width $\Delta(\omega_\nu) = \max\{0.4\ \text{MeV}, (\omega_\nu - 8\ \text{MeV})/3)\}$, for details see [23]. Further, Ψ_0 is the RPA ground state (g.s.) while ν runs over the RPA spectrum with eigenfrequencies ω_ν and eigenstates $|\Psi_\nu\rangle$. The $\hat{M}_\alpha(E1\mu)$ is the transition operator of the type $\alpha = \{E1, \text{tor,com}\}$.

For $E1(T = 1)$ transitions ($\alpha \equiv E1$), we consider the ordinary $E1$ operator ($\propto rY_{1\mu}$) with effective charges $e_1^p = N/A$ and $e_1^n = -Z/A$ and the strength (1) is weighted by the energy, i.e., $l = 1$. For $\alpha = \{\text{tor, com}\}$, we implement $e_0^p = e_0^n = 1$ for $T = 0$ ($e_1^p = -e_1^n = 1$ for $T = 1$) and no energy weight ($l = 0$).

The TR and CR operators used in Eq. (1) read [12]

$$\hat{M}_{\text{tor}}(E1\mu) = -\frac{1}{10\sqrt{2}c}\int d^3r\left[r^3 - \frac{5}{3}r\langle r^2\rangle_0\right] \times \vec{Y}_{11\mu}(\hat{\vec{r}})\cdot(\vec{\nabla}\times\hat{\vec{j}}_c(\vec{r})), \quad (2)$$

$$\hat{M}_{\text{com}}(E1\mu) = -\frac{i}{10c}\int d^3r\left[r^3 - \frac{5}{3}r\langle r^2\rangle_0\right] \times Y_{1\mu}(\hat{\vec{r}})\,(\vec{\nabla}\cdot\hat{\vec{j}}_c(\vec{r})), \quad (3)$$

where $\hat{\vec{j}}_c(\vec{r})$ is operator of the convection nuclear current, $\vec{Y}_{11\mu}(\hat{\vec{r}})$ and $Y_{1\mu}(\hat{\vec{r}})$ are vector and ordinary spherical harmonics. The terms with the g.s. squared radius $\langle r^2\rangle_0 = \int d^3r\, r^2\rho_0(\vec{r})/A$ account for the c.m.c., $\rho_0(\vec{r})$ is the g.s. density. Note that we describe CR and TR operators on the same footing using the current $\hat{\vec{j}}_c$. There is the direct relation [12] $\hat{M}_{\text{com}}(E1\mu) = -\hat{M}'_{\text{com}}(E1\mu)\omega/(\hbar c)$ between the CR current-dependent operator (3) and its familiar density-dependent counterpart

$$\hat{M}'_{\text{com}}(E1\mu) = \frac{1}{10}\int d^3r\,\hat{\rho}(\vec{r})\left[r^3 - \frac{5}{3}\langle r^2\rangle_0 r\right]Y_{1\mu}(\hat{\vec{r}}), \quad (4)$$

where $\hat{\rho}(\vec{r})$ is the density operator.

The operators (2)–(4) are derived as second-order $\sim r^3Y_{1\mu}$ terms in the low-momentum expansion of the ordinary $E1$ transition operator [8,9,12]. Despite their second-order origin, TR and CR dominate in the $E1(T = 0)$ channel where the leading c.m. motion driven by the operator $rY_{1\mu}$ is removed as the spurious mode. Following Eqs. (2) and (3), TR and CR deliver information on the curl $\vec{\nabla}\times\hat{\vec{j}}_c$ and divergence $\vec{\nabla}\cdot\hat{\vec{j}}_c$ of the nuclear current. As shown in [12], the corresponding velocity operators indicate that TR is purely vortical and CR is irrotational.

III. RESULTS AND DISCUSSION

Results of the calculations are given in Figs. 2–7. In Fig. 2, the strength functions (1) are shown. In panel (a), we see a good agreement of the computed giant dipole resonance (GDR) with the experiment [24], which confirms the accuracy of our description. For the LES region 6–10.5 MeV (marked as pygmy), we get two peaks at 7.5 and 10.3 MeV in accordance

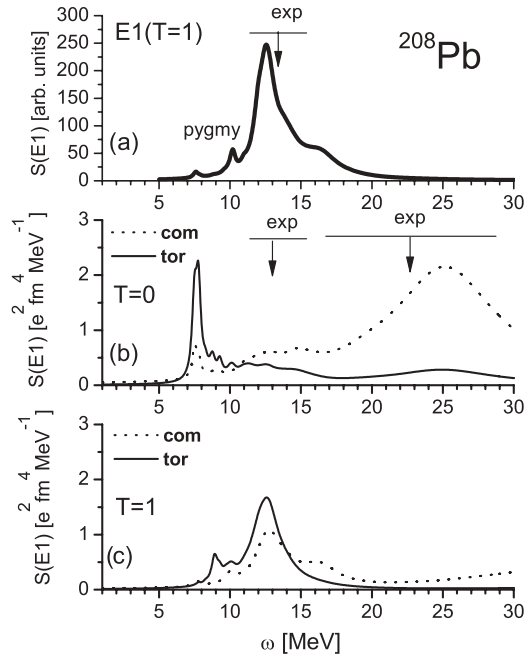

FIG. 2. Strength functions calculated within RPA with the force SLy6. (a) $E1(T=1)$ giant resonance. The line and arrow indicate the experimental width and energy centroid of the resonance [24]. The pygmy region is marked. (b) Toroidal (solid line) and compression (dotted line) $E1(T=0)$ strengths. The widths and energy centroids of the low- and high-energy branches of ISGDR observed in the (α,α') reaction [25] are denoted. (c) The same as in the plot (b) but in the $T=1$ channel.

with previous RMF calculations [4]. Panels (b) and (c) show TR and CR strengths in $T=0$ and $T=1$ channels. For $T=0$, the TR and CR are believed to constitute the low- and high-energy parts of the ISGDR [1]. Our results somewhat deviate from the experimental (α,α') data [25], but a similar discrepancy takes place in almost all theoretical studies [1]. Perhaps, at 12–14 MeV not the TR but the low-energy CR bump [see panel b)] is observed. The discrepancy for the high-energy CR may be caused by its sensibility to the calculation scheme. What is important for our aims, the LES region should certainly host the dominant and strongly peaked part of TR($T=0$), the left flank of TR($T=1$), and a non-negligible low-energy fraction of CR. In other words, we expect here a complicated interplay of several modes.

To understand the LES structure, we need more detailed observables than the strength distribution. In the following, we will consider transition densities (TD) $\delta\rho_\nu(r)=\langle\Psi_\nu|\hat\rho|\Psi_0\rangle$ and current transition densities (CTD) $\delta\vec j_\nu(\vec r)=\langle\Psi_\nu|\hat{\vec j}_c|\Psi_0\rangle$ (analogous to velocity fields). As we have in ^{208}Pb a high density of states, it is not worth to look at the pattern of individual states ν, which can vary from state to state and so hide common features of the flow. Thus we will consider transition densities and velocity fields averaged over given energy intervals. Incoherent averaging requires expressions which are bilinear in the excited states $|\Psi_\nu\rangle$. This is achieved by summing TD and CTD weighted by the matrix elements

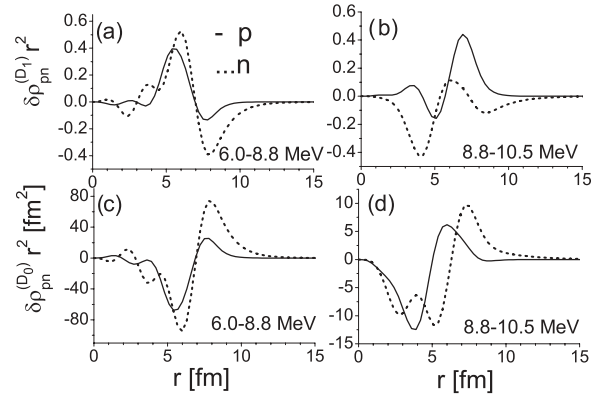

FIG. 3. Summed r^2-weighted proton and neutron TD $\delta\rho^{(D_1)}_{p,n}$ (a),(b) and $\delta\rho^{(D_0)}_{p,n}$ (c),(d) at the energy intervals 6.0–8.8 MeV (left) and 8.8–10.5 MeV (right).

$D_{T\nu}=\langle\nu|\hat D_T(E1)|0\rangle$ of a probe operator $\hat D_T(E1)$:

$$\delta\rho^{(D)}_\beta(\vec r)=\sum_{\nu\in[\omega_1,\omega_2]}D^*_{T\nu}\sum_{q=n,p}e^q_\beta\delta\rho^q_\nu(\vec r), \tag{5}$$

$$\delta\vec j^{(D)}_\beta(\vec r)=\sum_{\nu\in[\omega_1,\omega_2]}D^*_{T\nu}\sum_{q=n,p}e^q_\beta\delta\vec j^q_\nu(\vec r). \tag{6}$$

The sums in Eqs. (5) and (6) involve all the RPA states $|\nu\rangle$ in the energy interval $[\omega_1,\omega_2]$. For LES two energy intervals (with essentially different LES structure), 6.0–8.8 MeV with 7 states and 8.8–10.5 MeV with 13 states, are considered. Since states ν contribute twice (to $D^*_{T\nu}$ and transition densities $\delta\rho^q_\nu/\,\delta\vec j^q_\nu$), the expressions are independent of the phase of each state $|\Psi_\nu\rangle$ as it should be. In Eqs. (5) and (6), the index $\beta=p,n,0,1$ defines the type of TD or CTD (neutron, proton, $T=0$, $T=1$) by the proper choice of the effective charges: $e^p_p=1$, $e^n_p=0$; $e^p_n=0$, $e^n_n=1$; $e^p_0=e^n_0=1$; $e^p_1=N/A$, $e^n_1=-Z/A$. We use two different dipole probe operators: the isovector $\hat D_1=(N/A)\sum_i^Z(rY_1)_i-(Z/A)\sum_i^N(rY_1)_i$ relevant for reactions with photons and electrons, and isoscalar compressional $\hat D_0=\sum_i^A(r^3Y_1)_i$ relevant for (α,α') reaction. Due to $D^*_{T\nu}$ weights, the contribution of RPA states with a large D_T strength is enhanced.

In Fig. 3, the TD summed over two bins of the LES, 6.0–8.8 MeV and 8.8–10.5 MeV, are shown. One sees that, up to a scale factor, the TD for the probes D_1 and D_0 are rather similar, especially at 6.0–8.8 MeV. Panels (a) and (c) show that at 6.0–8.8 MeV the protons and neutrons oscillate in phase in the interior area 4–7 fm (isoscalar flow of the core) but neutrons dominate at larger distances $r>7$ fm (contribution of the neutron excess). Due to the r^2 factor, mainly the surface area $r>7$ fm contributes to the $B(E1)\propto\int dr r^2\delta\rho(r)$. This would favor the simple PDR picture of neutron-core oscillations. At the higher energy, 8.8–10.5 MeV, we see mainly isovector motion at 6–8 fm and again dominance of neutrons at $r>8$ fm. So, LES here is more isovector and does not support the PDR picture. Furthermore, the isoscalar D_0 leads to much weaker TD at 8.8–10.5 MeV relative to the region 6.0–8.8 MeV. This is probably caused by the fact that LES at 6.0–8.8 MeV is mainly isoscalar. Note that the r^2 factor amplifies the pattern in the nuclear surface and damps it in the interior area at

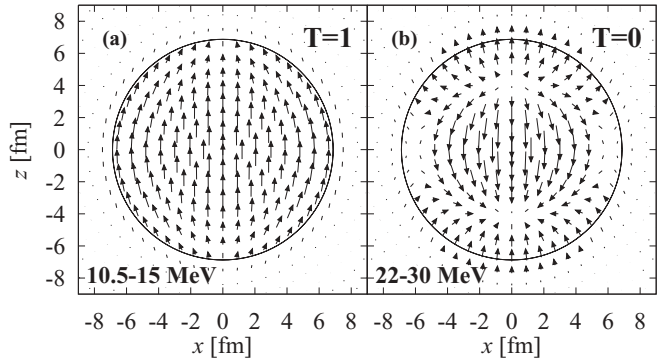

FIG. 4. Summed CTD (a) $\delta\vec{j}_1^{(D_1)}$ for GDR in the bin 10.5–15 MeV and (b) $\delta\vec{j}_0^{(D_0)}$ for CR($T=0$) in the bin 22–30 MeV.

$r < 4$ fm. The TD in Fig. 3 indicate that there are sizable effects in the interior. This will be corroborated by the flow pictures below.

A thorough analysis of excitations should also look at CTD which reveal more details than mere TD. The CTD for dipole states $\lambda\mu = 10$ are presented in Figs. 4–7. In Fig. 4, the fields for the isovector GDR (10.5–15 MeV) and high-energy isoscalar CR (22–30 MeV) are given as reference examples. They show typical GDR and CR flows, see [14,26,27] for a comparison. In the CR case, the compression and decompression zones along the z-axis are visible, as in Fig. 1(c). These plots for well-known modes serve as a benchmark and assert the validity of our prescription.

In Figs. 5–7 the fields for the two LES bins, 6.0–8.8 and 8.8–10.5 MeV, are depicted. Since D_1 and D_0 fields look, up to a scale factor, rather similar (especially for the bin 6.0–8.8 MeV), we will show further on only D_1 weighted CTD. In

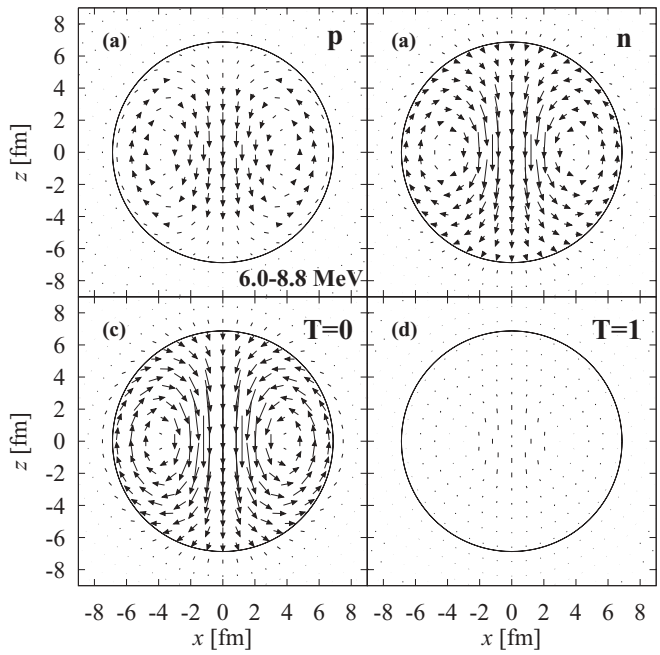

FIG. 5. Proton (a), neutron (b), $T = 0$ (c), and $T = 1$ (d) summed CTD $\delta\vec{j}_\beta^{(D_1)}$ in the bin 6.0–8.8 MeV.

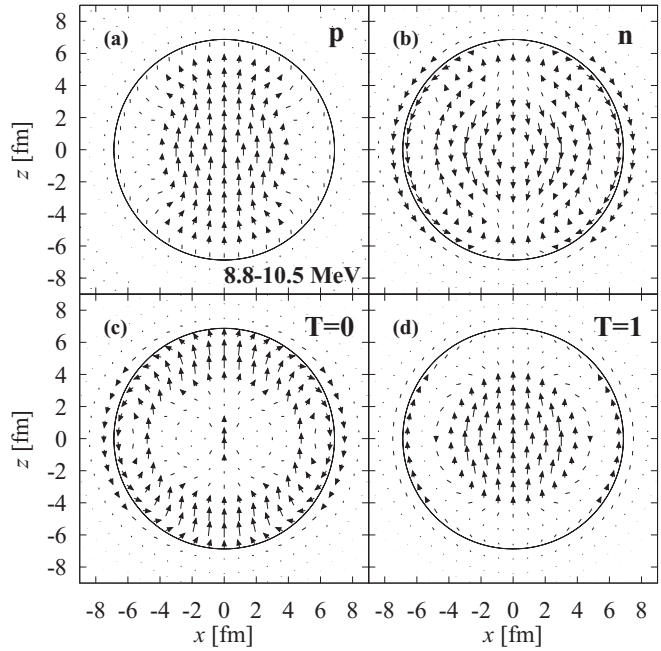

FIG. 6. The same as in Fig. 5 but for the bin 8.8–10.5 MeV.

every figure, the actual CTD scale (common for all the plots) is adjusted for better view. Arbitrary units for CTD are used.

Figure 5 shows the fields in the bin 6.0–8.8 MeV. The neutron flow dominates in both interior and surface. Since protons and neutrons move in phase, the total flow is essentially isoscalar, see panels (c) and (d) in comparison. The $T = 0$ character of the lower bin of LES is in accordance with previous theoretical results [4,28] and experimental findings, e.g., for ^{124}Sn [29]. What is important for our aims, Fig. 5 clearly demonstrates the overwhelming toroidal flow in neutron and $T = 0$ cases (less in the proton case). This is in accordance with the TR($T = 0$) strength from Fig. 2(b), which is strictly peaked just at 7–8 MeV and dominates over the CR($T = 0$). Therefore, LES at 6.0–8.8 MeV is of almost pure toroidal (vortical) nature. The irrotational PDR flow is not seen at all.

The LES fields in the bin 8.8–10.5 MeV in Fig. 6 are more complicated. The flow is mainly isovector in the nuclear interior and isoscalar at the surface, thus demonstrating an isospin-mixed character (again in accordance to RMF findings [4,28]). Furthermore, the TR flow is faint. Actually there are hints of several flows: TR (b),(c), CR (b), and familiar linear dipole (a),(d). This complex picture reflects the fact that, following Figs. 2(b) and 2(c), the region 8.8–10.5 MeV hosts various modes and feels already the vicinity to the GDR.

Finally, Fig. 7 exhibits the r^2-weighted CTD to highlight the role of surface nucleons (e.g., the neutron excess) in the peripheral reactions like (α, α') and, to a lesser extent, photoabsorption. Flows in Fig. 7 correspond to the TD in Fig. 3 (a),(b). The r^2-weighted presentation weakens the interior flow and emphasizes the role of the neutron excess, see Fig. 7(b). Nevertheless, the LES still keeps their TR and mixed (TR/CR) nature in the bins 6.0–8.8 and 8.8–10.5 MeV. Again we cannot find any sizable evidence for PDR flow.

In our calculations, the LES contributions to the TRK sum rule are 1.1% and 3.3% for the intervals 6.0–8.8 and

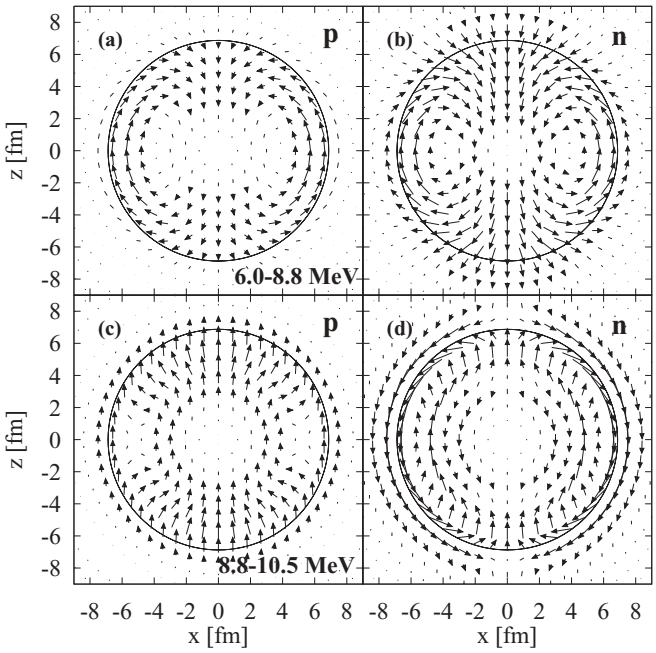

FIG. 7. The r^2-weighted proton and neutron $\delta\vec{j}_\beta^{(D_1)}$ in the bins 6.0–8.8 MeV (a),(b) and 8.8–10.5 MeV (c),(d).

8.8–10.5 MeV, respectively. The total amount 4.4% is in accordance to previous theoretical and experimental studies [1]. Our results are also in a good agreement with findings [14]. We get the peaked $E1$ strength at ∼7.5 MeV (found in [14] in both experiment and theory). Our TD and CTD well agree with those of [14] obtained with the CCC. In particular, our transition densities at 6.0–8.8 MeV [Fig. 2 (a),(c)] are very similar to those of [14] at 7–8 MeV. Moreover, at 6–8.8 MeV we get the average toroidal velocity fields analogous to that of [14] at 6.5–10.5 MeV. At the same time, unlike [14] and in accordance to the previous studies [4,28,29], we found a more complicated LES structure: isoscalar toroidal low-energy part and mixed isoscalar/isovector toroidal/compression high-energy part. In this study we do not take into account the CCC which in general may be essential for LES [29–31]. However the LES features, we have found, are too strong to be spoiled by this effect. Note also that the TR/PDR interplay was recently discussed in the semiclassical study [32] which also predicted the isoscalar toroidal flow in the LES region

The question remains how to observe the velocity fields experimentally and thus disclose the true nature of LES. The typical reactions mentioned above are mainly sensitive to the nuclear surface and lose the important information on the nuclear interior. This is especially the case for the isoscalar (α, α') whose response is driven by the operator r^3Y_1 with a huge surface enhanced factor. [Note also that the most relevant (α, α') measurements of ISGDR in ^{208}Pb [25] consider the energy interval $\omega > 8$ MeV and so, following our calculations, lose the TR($T = 0$) peaked at 7–8 MeV.] Perhaps, the (e, e') reaction which can cover both nuclear surface and interior is the most promising tool to examine LES flows.

IV. CONCLUSIONS

Self-consistent Skyrme-RPA calculations have been performed to inspect the nature of the $E1$ low-energy strength (LES), often denoted as the pygmy dipole resonance (PDR) and associated with the picture that the neutron skin oscillates against the nuclear core. Strength functions, averaged transition densities, and averaged current fields (collecting contributions of all RPA states in a given energy interval) were used for the analysis. The current fields turned out to be most important to illustrate the LES flows. The results show that, in agreement with previous studies [4,28], LES may be divided into two energy regions, 6.0–8.8 MeV and 8.8–10.5 MeV in our case, where the lower one is basically isoscalar and the higher one is isospin-mixed.

What is most interesting, LES at 6.0–8.8 MeV shows a clear toroidal (vortical) nature while the interval 8.8–10.5 MeV gives a mixed toroidal/compression/linear flow. No convincing indicator of PDR-like flow is found. This means that the familiar treatment of LES as the out-of-phase motion of the neutron excess against the nuclear core (arising from the analogy with light halo nuclei and suggested from r^2-weighted transition densities) is misleading. Our study does not deny the important contribution of the neutron excess to various (basically peripheral) reactions. At the same time, we find that LES flow pattern is far from a simple PDR picture and actually involves various types of motion, irrotational (compression) and vortical (toroidal). In particular, LES at 6.0–8.8 MeV constitutes an almost pure toroidal $T = 0$ resonance. This conclusion may have far-reaching consequences for further exploration of LES and related observables.

ACKNOWLEDGMENTS

The work was partly supported by the GSI-F+E-2010-12, Heisenberg-Landau (Germany - BLTP JINR), and Votruba-Blokhintsev (Czech Republic - BLTP JINR) grants. P.-G.R. is grateful for the BMBF support under Contracts No. 06 DD 9052D and No. 06 ER 9063. The support of the research plan MSM 0021620859 (Ministry of Education of the Czech Republic) and the grant of Czech Science Foundation (13-07117S) are appreciated.

[1] N. Paar, D. Vretenar, E. Khan, and G. Colo, Rep. Prog. Phys. **70**, 691 (2007).
[2] A. Carbone, G. Colo, A. Bracco, L. G. Cao, P. F. Bortignon, F. Camera, and O. Wieland, Phys. Rev. C **81**, 041301(R) (2010).
[3] P. Van Isacker, M. A. Nagarajan, and D. D. Warner, Phys. Rev. C **45**, R13 (1992).
[4] D. Vretenar, N. Paar, P. Ring, and G. A. Lalazissis, Phys. Rev. C **63**, 047301 (2001).
[5] X. Roca-Maza, G. Pozzi, M. Brenna, K. Mizuyama, and G. Colo, Phys. Rev. C **85**, 024601 (2012).
[6] E. Yuksel, E. Khan, and K. Bozkurt, Nucl. Phys. A **877**, 35 (2012).

[7] P.-G. Reinhard and W. Nazarewicz, arXiv:1211.1649v1 [nucl-th].
[8] V. M. Dubovik and A. A. Cheshkov, Sov. J. Part. Nucl. **5**, 318 (1975).
[9] S. F. Semenko, Sov. J. Nucl. Phys. **34**, 356 (1981).
[10] M. N. Harakeh, K. van der Borg, T. Ishimatsu, H. P. Morsch, A. van der Woude, and F. E. Bertrand, Phys. Rev. Lett. **38**, 676 (1977).
[11] S. Stringari, Phys. Lett. B **108**, 232 (1982).
[12] J. Kvasil, V. O. Nesterenko, W. Kleinig, P.-G. Reinhard, and P. Vesely, Phys. Rev. C **84**, 034303 (2011).
[13] J. Kvasil, A. Repko, V. O. Nesterenko, W. Kleinig, P.-G. Reinhard, and N. Lo Iudice, arXiv:1211.2978 [nucl-th].
[14] N. Ryezayeva, T. Hartmann, Y. Kalmykov, H. Lenske, P. von Neumann-Cosel, V. Yu. Ponomarev, A. Richter, A. Shevchenko, S. Volz, and J. Wambach, Phys. Rev. Lett. **89**, 272502 (2002).
[15] D. G. Ravenhall and J. Wambach, Nucl. Phys. A **475**, 468 (1987).
[16] N. Lyutorovich, V. I. Tselyaev, J. Speth, S. Krewald, F. Grümmer, and P. G. Reinhard, Phys. Rev. Lett. **109**, 092502 (2012).
[17] P.-G. Reinhard, Ann. Physik **1**, 632 (1992).
[18] T. H. R. Skyrme, Phil. Mag. **1**, 1043 (1956).
[19] D. Vauterin and D. M. Brink, Phys. Rev. C **5**, 626 (1972).
[20] M. Bender, P.-H. Heenen, and P.-G. Reinhard, Rev. Mod. Phys. **75**, 121 (2003).
[21] E. Chabanat, P. Bonche, P. Haensel, J. Meyer, and R. Schaeffer, Nucl. Phys. A **635**, 231 (1998).
[22] W. Kleinig, V. O. Nesterenko, J. Kvasil, P.-G. Reinhard, and P. Vesely, Phys. Rev. C **78**, 044313 (2008).
[23] J. Kvasil, V. O. Nesterenko, W. Kleinig, D. Božík, and P.-G. Reinhard, Int. J. Mod. Phys. E **20**, 281 (2011).
[24] A. V. Varlamov *et al.*, Atlas of Giant Dipole Resonances, INDC(NDS)-394, 1999.
[25] M. Uchida *et al.*, Phys. Rev. C **69**, 051301(R) (2004).
[26] S. Misicu, Phys. Rev. C **73**, 024301 (2006).
[27] D. Vretenar, A. Wandelt, and P. Ring, Phys. Lett. B **487**, 334 (2000).
[28] N. Paar, Y. F. Niu, D. Vretenar, and J. Meng, Phys. Rev. Lett. **103**, 032502 (2009).
[29] J. Endres *et al.*, Phys. Rev. Lett. **105**, 212503 (2010).
[30] E. Litvinova, P. Ring, and V. Tselyaev, Phys. Rev. C **78**, 014312 (2008).
[31] N. N. Arsenyev, A. P. Severyukhin, V. V. Voronov, and Nguen Van Giai, arXiv:1209.6146 [nucl-th].
[32] M. Urban, Phys. Rev. C **85**, 034322 (2012).